Journal of Mines, Metals and Fuels, *73(3): 641-649; 2025. DOI: 10.18311/jmmf/2025/48074*

Print ISSN : 0022-2755

Journal of Mines, Metals and Fuels

**Contents available at:** *www.informaticsjournals.co.in/index.php/jmmf*

# Characterization of Microstructure and Mechanical Properties in Incoloy 925 and Inconel 625 Dissimilar Friction Stir Welds

**Varalakshmi Penugonda[1,2], G. Murali[1]*, Vijaya Kumar Bongarala[2], T. Jayasriram[2] and Anant Sidhappa Kurhade[3]**

*[1]Department of Mechanical Engineering, Koneru Lakshmaiah Education Foundation, Guntur - 522502, Andhra Pradesh, India; muralinitt@gmail.com*

*[2]Department of Mechanical Engineering, Guru Nanak Institute of Technology, Hyderabad - 501506, Telangana, India*

*[3]Department of Mechanical Engineering, Dr. D. Y. Patil Institute of Technology, Pimpri - 411018, Pune, Maharashtra, India*

## Abstract

*This study investigated the feasibility of joining Incoloy 925 and Inconel 625, two high-performance nickel-based alloys, using Friction Stir Welding (FSW). Various process parameters were examined, with tool rotation speeds between 300 and 500 rpm and welding speeds ranging from 20 to 100 mm/min. Satisfactory welds were consistently achieved at welding speeds of 20, 25, and 30 mm/min while maintaining a constant tool rotation speed of 400 rpm. Microstructural analysis identified four distinct zones within the weld: the base metal, Heat-Affected Zone (HAZ), Thermo-Mechanically Affected Zone (TMAZ), and Stir Zone (SZ). Interestingly, a well-defined HAZ was absent, likely due to rapid cooling during FSW and the inherent thermal properties of the alloys. The SZ exhibited dynamic recrystallization, producing a fine-grained microstructure, while minimal changes were noted in the TMAZ. X-ray diffraction confirmed no phase transformations or significant oxidation in the welded alloys. Microhardness measurements showed an asymmetric distribution, with hardness increasing from the base metal to the SZ. This was attributed to grain refinement and strengthening mechanisms within the SZ. Tensile testing revealed that Inconel 625 had inherently higher yield and tensile strengths than Incoloy 925. However, at a welding speed of 30 mm/min, the weld metal exhibited tensile strength comparable to the base metal of Incoloy 925. A slight reduction in elongation was observed, likely due to the differing deformation behaviours of the alloys.*

***Major Findings:*** *This study demonstrated the feasibility of joining Incoloy 925 and Inconel 625 using Friction Stir Welding (FSW), achieving optimal welds at speeds of 20–30 mm/min with a rotation speed of 400 rpm. The stir zone exhibited dynamic recrystallization, fine-grained microstructures, and increased hardness due to grain refinement. Tensile strengths comparable to the base metals and improved mechanical properties highlight the potential of FSW for high-temperature applications.*

**Keywords:** *Dynamic Recrystallization, Friction Stir Welding, Mechanical Properties, Microstructure, Nickel Alloys, X-ray Diffraction*

*Author for correspondence*

## 1.0 Introduction

The joining of dissimilar materials has been increasingly gaining attention across a range of industrial applications, due to its multifaceted advantages. The benefits extend beyond just technical merits in terms of product properties, but also to economic benefits in terms of production processes[1]. As a result, reliable techniques for joining dissimilar materials are getting more and more important. When joining metals with different chemical and physical compositions, traditional fusion welding methods have a lot of trouble. Due to this inherent challenge, solid-state joining methods are a central focus of research and development[2–8]. In recent years, there has been a notable increase of interest and focus directed toward the revolutionary welding technique known as Friction Stir Welding (FSW). FSW, which initially received a patent from The Welding Institute (TWI) in the UK[9], has proven to be extremely effective, especially when working with materials that have historically presented challenges in conventional fusion welding. High-strength magnesium and aluminum alloys are among these materials[10]. As a result, researchers have concerted efforts to broaden the applicability of FSW to include dissimilar alloy combinations. This ambitious endeavor has entailed welding materials as different as aluminum to steel, aluminum to magnesium, and aluminum to copper, among other combinations[11–17]. FSW, as an innovative solid-state joining technology, holds great promise for creating high-quality welds between materials that are traditionally challenging to unite through conventional fusion welding methods. However, it is important to acknowledge that, despite these advancements, previous studies have unveiled a set of distinct challenges when it comes to achieving robust dissimilar FSW joints. Typically, these joints tend to exhibit failure at the nugget or along the interface between the two materials during rigorous mechanical testing. This revelation underscores the pressing need for a comprehensive examination of the microstructures within the nugget and along the bonding interface of dissimilar FSW joints. Such research endeavors are invaluable in providing insights into the myriad factors that influence the integrity of these joints. Furthermore, they offer a pathway toward enhancing the FSW process, ultimately ensuring its success in facilitating high-quality and reliable welds between dissimilar materials in an ever-expanding range of industrial applications[18]. The Inconel 625 alloy is commonly utilized in chemical power plants, aerospace systems, and maritime systems because of its outstanding qualities, which include high tensile strength, extraordinary corrosion resistance, and great fabricability. Because molybdenum and niobium give the nickel-chromium matrix in this alloy strength, it is noteworthy that it is a solid solution-strengthened material. The special benefit is that it may maintain high strength without requiring heat treatment to cause precipitation. Inconel 625 also exhibits precipitation hardening at high temperatures, which leads to the development of precipitates such γ', γ" and several carbides (MC, $M_6C$, and $M_{23}C_6$). Usually, fusion-welding techniques like Gas Tungsten Arc Welding (GTAW) and laser welding have been used to repair power generator components and build chemical power plants using Ni-based alloys like Inconel 625. Nevertheless, it might be difficult to get the ideal physical and chemical characteristics in the weld zone since these fusion welds frequently result in the creation of a cast structure. This study suggests Friction Stir Welding (FSW), an alternate welding technique, in recognition of this difficulty. FSW is selected because, of its reduced heat input, it can keep the material in a solid state, potentially resolving the drawbacks of conventional fusion welding techniques[19,20]. On the other side, with a lower nickel concentration than Inconel 625 and Inconel 718 grades, Incoloy 925 distinguishes out as a precipitation-hardened and age-hardenable superalloy. Modest additions of alloying elements including Molybdenum, Copper, Aluminum, and Titanium are included in Incoloy 925 alloy. Despite its reduced nickel levels, Incoloy 925 maintains significant resistance to chloride-ion stress corrosion cracking. Incoloy 825 and 925 are both resistant to cracking in hydrogen sulfide, as demonstrated by DuPont *et al.*'s very slow rates of fracture formation in slow strain rate tests[21]. Notably, Incoloy 925 is used in the petrochemical industry as a potential metal for vacuum-insulated double-wall tubing (VIT). In the extraction process, when cooling is inherent, this use is critical to preventing a rise in crude oil viscosity. The alloy is ideal for a variety of applications in the sour gas, oil, and marine sectors due to its remarkable combination of mechanical strength and general corrosion resistance[22]. Numerous studies on the friction stir welding of Ni-based alloys have been published in recent times. Friction

stir welding for Inconel 600 has been shown by Song et al. to produce perfect welds at lower speeds and to produce grain refinement by dynamic recrystallization[23]. The gradual refining of the grain as the welding speed increases reveals a parameter that may be controlled. The welded zone has a ten percent greater tensile strength and a twenty percent higher microhardness than the base material, indicating that the technique significantly enhances the mechanical properties. In addition, Song and Nakata explored Friction Stir Welding (FSW) of 2 mm thick sheets of Inconel 625, utilizing WC–Co tool material. Their findings highlighted enhanced mechanical properties, including increased microhardness and tensile strength in the welds, attributed to grain refinement, when compared to the base materials[24]. Successful friction stirs welding of precipitation-strengthened Haynes 282 nickel alloy was achieved by Mageshwari Komarasamy *et al.,* producing welds that lack defects with lower rotational speeds. The processed region exhibited a welded microstructure with finely divided grains, with the finest grain size in the processed condition[25]. The cross-weld tensile characteristics were reduced by less than three percent while still identical to the base metal. Radha Krishnan Beemaraj *et al.* proposed a dissimilar welding method for Inconel alloys in the Friction Stir Welding process. Their study focused on Inconel 600 and Inconel 718, using rotating grating welding to achieve quality welds, and revealed robust joint performance in the Inconel 718 heat-affected zone, demonstrating high ultimate tensile strength and satisfactory ductility[26].

To our knowledge, Inconel 625 and Incoloy 925 alloy dissimilar friction stir welding have never been in the available literature. This study aims to investigate the feasibility and characterize the mechanical and microstructural properties of Friction Stir Welded (FSW) joints between Incoloy 925 and Inconel 625, two high-performance nickel-based alloys. The study will explore the influence of process parameters, such as tool rotation speed and welding speed, on the quality and integrity of the FSW joints.

## 2.0 Materials and Methods

### 2.1 Materials

Inconel 625 and Incoloy 925 alloy sheets were used for friction stir welding, with dimensions of 105 x 80 x 2

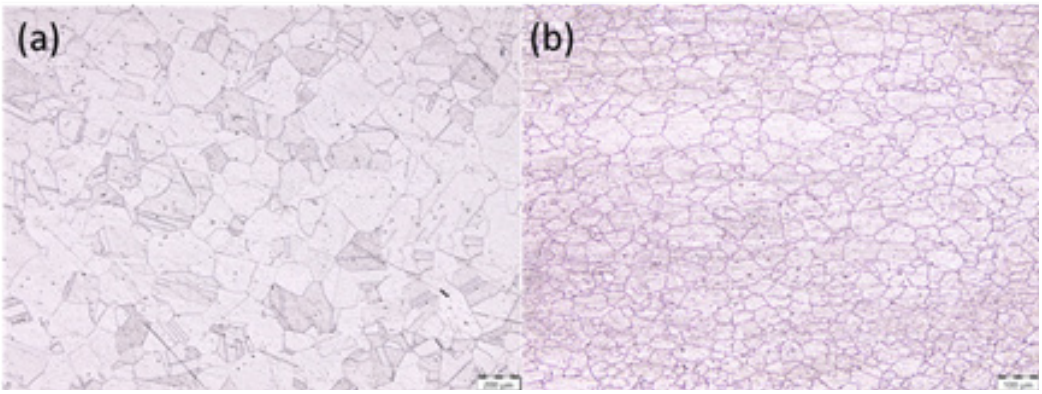



**Figure 1.** **(a)** Incoloy 925 base metal **(b)** Inconel 625 base metal.

**Table 1.** The elemental composition of Incoloy 925 and Inconel 625

| Material | Ni | Cr | Fe | Mo | Cu | W | Co | Ti | Al | Mn | Si | Nb | V | C | S |
|---|---|---|---|---|---|---|---|---|---|---|---|---|---|---|---|
| Incoloy 925 | Bal | 19.5-22.5 | 22.0 | 2.5-3.5 | 1.5-3.0 | ---- | ---- | 1.9-2.4 | 0.1-0.5 | 1.0 | 0.5 | 0.5 | ---- | 0.03 | 0.03 |
| Inconel 625 | Bal | 20.0-22.5 | 2.0-6.0 | 12.5-14.5 | ---- | 2.5-3.5 | 2.5 | ---- | ---- | 0.50 | 0.08 | ---- | 0.35 | 0.015 | 0.02 |

mm. The composition of Inconel 625 and Incoloy 925 are provided in Table 1. The microstructure of Incoloy 925 and Inconel 625 is shown in Figure 1.

### 2.2 Experimental Methods

Figure 2 illustrates the experimental setup employed for Friction Stir Welding (FSW) and provides a schematic perspective of the process. Grain refinement within the FSW joint is significantly influenced by the rotational speed of the welding tool. In this study, a range of rotational speeds, including 300 rpm, 400 rpm, and 500 rpm, were investigated. A Tungsten Carbide Cobalt (WC-Co) tool was utilized, featuring a pin diameter of 6 mm, a shoulder diameter of 18 mm, and a pin length of 1.9 mm. Through systematic experimentation, optimal process parameters were identified: a rotational speed of 400 rpm, a traverse speed of 30 mm/min, and a tool tilt angle of 3 degrees. To prevent surface oxidation during the welding process, an argon gas shield was employed. The microstructural analysis involved preparing polished specimens and etching them using a solution of hydrochloric acid, nitric acid, and sulfuric acid. Interfacial microstructures were examined using an optical microscope (Olympus BX41M). X-Ray Diffraction (XRD) analysis was conducted using a Rigaku Miniflex 600 to assess the phase composition and crystal structure of the welded joint. Microhardness measurements were performed using a Vickers hardness tester to evaluate the hardness distribution within the weld. Tensile test specimens were prepared according to ASTM C749 standards and subsequently tested on a servo-controlled universal testing machine (FIE – BLUESTAR, INDIA, Model: UNITEK 94100) at a crosshead speed of 0.5 mm/min. To ensure data reliability, three tensile tests were conducted for each set of process parameters, and the average results were reported. All tensile tests were conducted by ASTM standards, utilizing a Universal testing machine with a 40 kN capacity and a loading rate of 1.5 kN/min.

## 3.0 Result and Discussions

Employing friction stir welding, this study explored Inconel 625 and Incoloy 925 sheets across a wide spectrum of tool rotation speeds (300-500 rpm) and welding speeds (20-100 mm/min). Consistently robust joints were achieved at a constant tool rotation speed of 400 rpm for welding speeds of 20, 25, and 30 mm/min. These samples were then utilized for an in-depth examination of the mechanical and microstructural properties inherent in the friction stir welding process applied to Inconel 625 and Incoloy 925 alloys.

### 3.1 Microscopic Analysis of Weld Joints

The illustration highlights Incoloy 925 as the advancing side, while Inconel 625 was on the retreating side. Following FSW, four well-defined regions emerge, namely the Base Metal (BM), the Heat-Affected Zone (HAZ), the Thermos-Mechanically Affected Zone (TMAZ), the nugget or Stirred Zone (SZ) (Figure 3). The microstructural characterization of Incoloy 925 parent

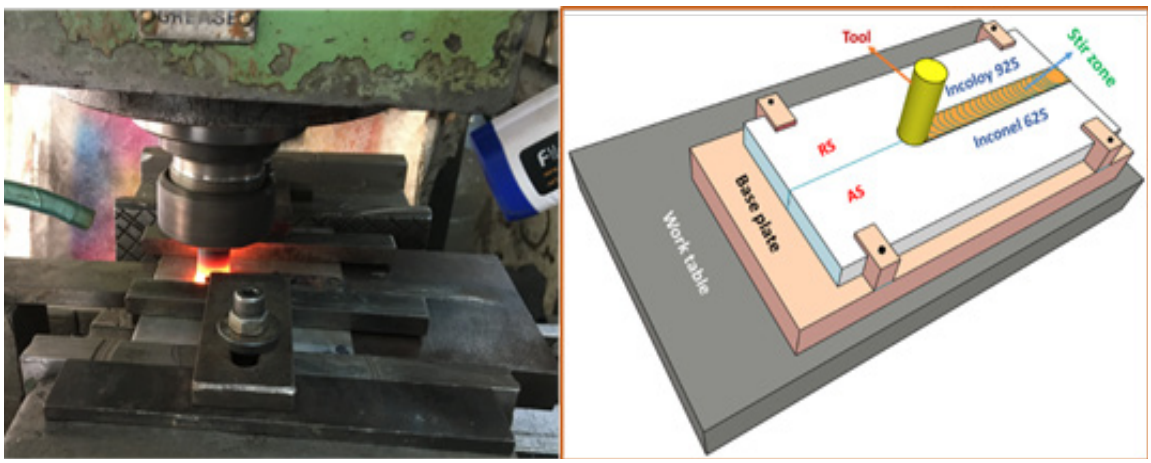



**Figure 2.** The experimental setup for Friction Stir Welding used in the welding process and the schematic illustration of the Friction Stir Welding arrangement.

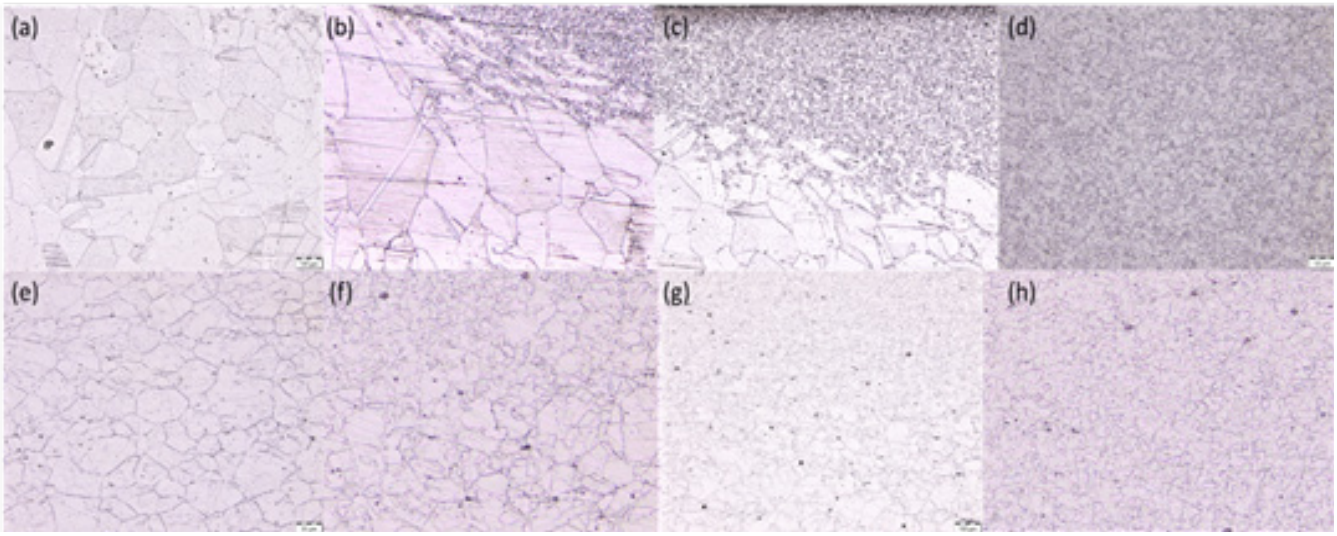



**Figure 3.** **(a)** 925 HAZ **(b)** 925 TMAZ **(c)** 925 side Interface between TMAZ and stir zone **(d)** 925 side Stir zone **(e)** 625 HAZ **(f)** 625 TMAZ **(g)** 625 side Interface between TMAZ and stir zone **(h)** 625 side Stir zone.

metal unveiled a single-phase austenitic microstructure with an average grain size of approximately 41 µM. Within this austenite matrix, cubic-shaped phases or precipitates were discerned, and identified through EDS analysis as titanium carbonitride (Ti (N, C) phases). This observation aligns coherently with existing literature, particularly a study characterizing Ti-rich phases in Incoloy 925. Furthermore, the presence of TiN inclusions in Ni-based superalloys, as reported by Busch *et al.,* corresponds to the current findings[27]. The higher susceptibility of Incoloy 925 to the formation of Ti (N, C) phases is attributed to its elevated titanium content compared to various grades of Ni-based superalloys. The investigation into microstructure dynamics unveiled a noteworthy absence of a distinct Heat-Affected Zone (HAZ) in both Incoloy 925 and Inconel 625 sides. This absence was attributed to the combined influence of the rapid cooling rate induced by Friction Stir Welding (FSW) and the intrinsic thermal properties of the parent metals. This outcome is consistent with earlier research, as highlighted by Song and Nakata[24], where a clear HAZ was not observed in FSW weldments. Subsequent analysis delved into the areas formed after the HAZ, distinguishing the Thermo-Mechanical Affected Zone (TMAZ) and Stir Zone (SZ). TMAZ, characterized by incomplete recrystallization, displayed elongated grains, fine equiaxed grains, twins, and serrated grain boundaries. Interestingly, across various FSW parameters, TMAZ microstructures remained similar, suggesting a minimal impact compared to the SZs. This inference aligns with the understanding that the microstructure of TMAZs is influenced by both thermal cycles and plastic deformation, primarily originating from the FSW tool. However, the SZs exhibited a fine-grain structure indicative of dynamic recrystallization mechanisms.

Dynamic Recrystallization (DRX) is a crucial process in FSW of nickel alloys. During FSW, intense friction generates localized heat, raising temperatures to levels sufficient to induce DRX, even below the melting point. This elevated temperature, combined with the severe plastic deformation caused by the rotating tool, creates ideal conditions for DRX to occur. DRX leads to the formation of new, smaller grains within the stir zone, resulting in a more refined and homogenous microstructure. This refined microstructure mitigates the effects of prior deformation and thermal cycling, ultimately enhancing the strength, hardness, and overall performance of the welded joint.

## 3.2 X-Ray Diffraction Analysis

XRD analysis was performed on the stir zone of Inconel 625 and Incoloy 925 after FSW. The XRD pattern, illustrated in Figure 4, exhibited diffraction peaks corresponding to the crystal structure of Inconel 625 and Incoloy 925, specifically from the (111), (200), and (220) planes. These peaks were consistently observed

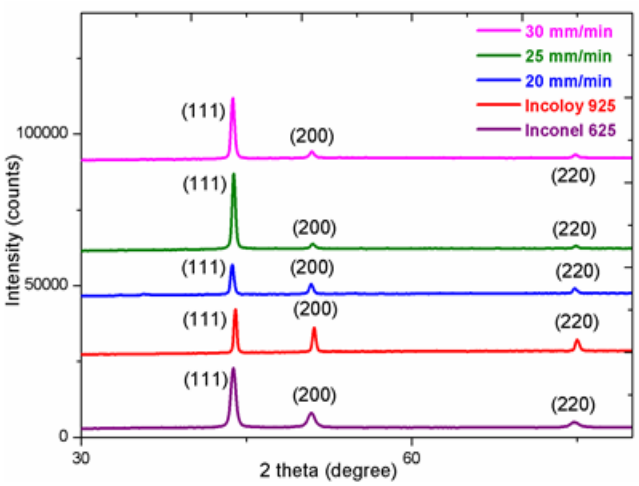



**Figure 4.** X-ray diffraction spectrum of as-received Inconel 625, Incoloy 925, friction stir welded Inconel 625, Incoloy 925 at 20 mm/min, 25 mm/min, and 30 mm/min traverse speed.

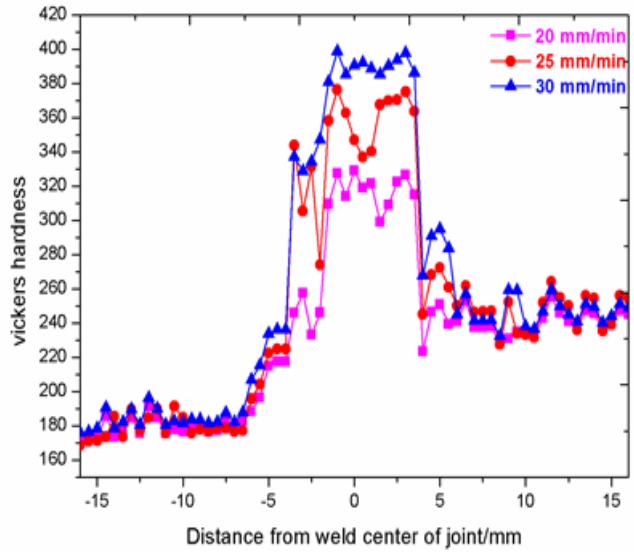



**Figure 5.** Distribution of Vickers hardness calculated during the midpoint perpendicular to the welding direction of FSW Inconel 625, Incoloy 925 at welding speeds of 20, 25, and 30 mm/min.

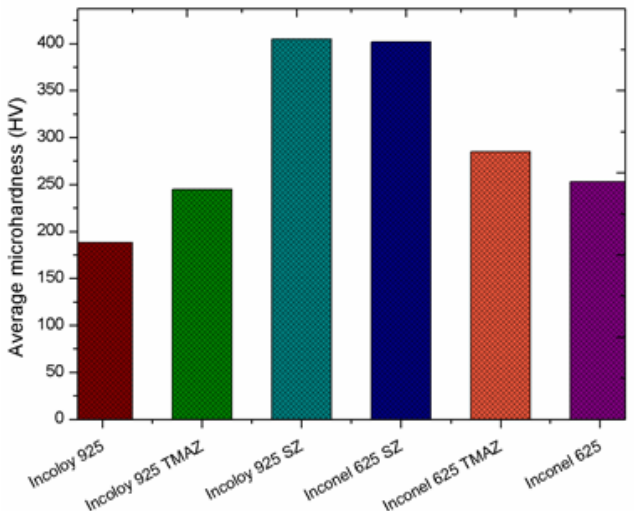



**Figure 6.** Average microhardness values of the dissimilar FSW Inconel 625, Incoloy 925, 30 mm/min sample (SZ: Stir Zone, TMAZ: Thermo-Mechanical Affected Zone).

at 0.5 mm from the center of the stir region on both the advancing and retreating sides of the cross-section. Crucially, no additional peaks were detected in the X-ray diffractogram, indicating that there were no changes in the phase or oxidation state of Inconel 625 and Incoloy 925 during the FSW process. This finding is significant, as any alterations in these properties could affect the mechanical properties of the materials. Therefore, the X-ray diffraction analysis confirmed that the FSW process did not induce any undesirable modifications in the material, ensuring the integrity and reliability of the welded component.

## 3.3 Microhardness Distribution

The microhardness profile was obtained by measuring the material at the center of the cross-section and along the line, with the results shown in Figure 5 and Figure 6. A clear asymmetry in the hardness distribution was observed, with hardness values rising from the base metal of Incoloy 925 (188 HV) to the TMAZ (245 HV), and further to the SZ of Incoloy 925 (405 HV). Similarly, hardness increased from the base metal of Inconel 625 (253 HV) to the TMAZ (285 HV), and then to the SZ of Inconel 625 (402 HV). The stir zones exhibited significantly higher hardness compared to the parent metals, with microhardness increasing as welding speed increased. At 20 mm/min, the SZ hardness was around 330 HV, rising to 380 HV at 25 mm/min, and reaching a peak of 405 HV at 30 mm/min, which improved tensile properties. This increase was attributed to grain size refinement resulting from dynamic recrystallization during stirring, by the Hall-Petch relationship. The smallest grain size in the nugget zone resulted in the highest hardness, while hardness decreased as the distance from the weld increased on both

the retreating and advancing sides. These results highlight the influence of the welding process on the mechanical properties of the joint.

## 3.4 Tensile Properties

The stress-strain curves, which are crucial for engineering analysis, are depicted in Figure 7, while detailed mechanical properties are outlined in Figure 8. The study's findings emphasize the superior performance of Inconel 625, which exhibited the highest yield strength (470 MPa) and tensile strength (914 MPa) among the tested materials. Notably, at a welding speed of 30 mm/min, the yield and tensile strengths were comparable to those of the Incoloy 925 base metal. However, in the transverse tensile test, the weld metal showed adequate strength but limited elongation (27%), significantly lower than the 49% observed in Inconel 625 and the 55% in Incoloy 925. This reduced elongation is attributed to incompatible deformation between the dissimilar materials. The Incoloy 925 base metal had a tensile strength of 695 MPa, while welding speeds of 20, 25, and 30 mm/min resulted in tensile strengths of 516, 626, and 685 MPa, respectively. The higher hardness of the stir zones suggests they remained undeformed during tensile tests.

As strength inversely correlates with hardness, the base metal likely failed during transverse tensile tests,

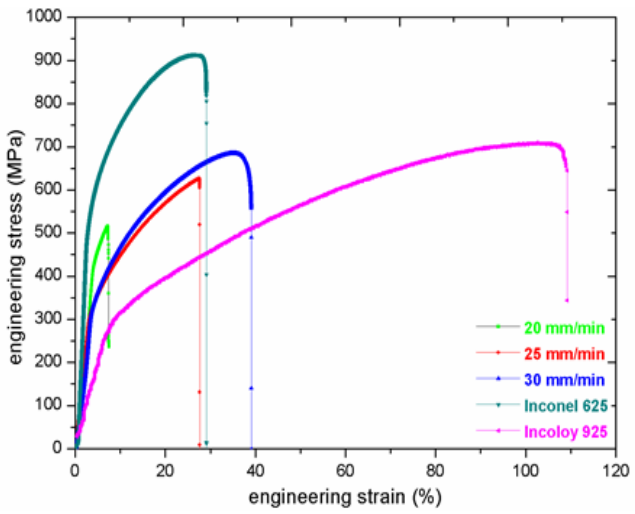



**Figure 7.** Engineering stress-strain curve of specimens milled in SZ of dissimilar FSW Inconel 625 Incoloy 925 alloys welded at the welding speeds 20, 25, and 30 mm/min and base metals.

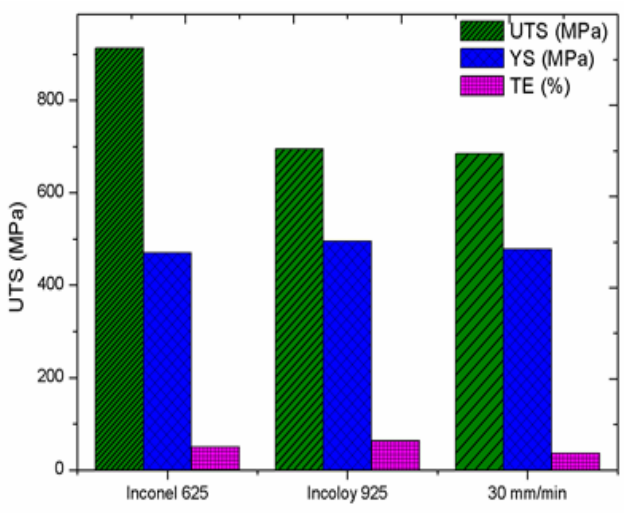



**Figure 8.** Mechanical properties of Inconel 625 Incoloy 925 alloys friction stir welded at the welding speed 30 mm/min and parent metals.

reducing overall engineering stress. Additionally, crack initiation in Incoloy 925 occurred before that in Inconel 625, concentrating distortion primarily on Incoloy 925 and reducing elongation. It is noteworthy that prior studies by other researchers have also shown lower elongation in friction stir weldments compared to parent metals. Although fractures originated from the root side during tensile testing, they did not propagate along material interfaces, indicating thorough mixing of the alloys and negating the interface as a weak point. The curvature of the weldment surface may have contributed to the root side fracture, as plastic deformation caused by the pressure from the tool, especially the shoulder, can result in curved plate surfaces during welding. This finding underscores the importance of considering not only the mechanical properties of the materials but also the welding process itself in evaluating the performance of friction stir weldments.

## 3.5 Quantitative Results from the FSW Study

| Parameter | Value/Result |
|---|---|
| Tool Rotation Speed (rpm) | 300, 400, 500 |
| Welding Speed (mm/min) | 20, 25, 30 |

| | |
|---|---|
| Base Metal Hardness (HV) | Incoloy 925: 188, Inconel 625: 253 |
| Microhardness of Stir Zone (HV) | At 20 mm/min: ~330, At 25 mm/min: 380, At 30 mm/min: 405 |
| Yield Strength (MPa) | Incoloy 925: 380, Inconel 625: 470 |
| Tensile Strength (MPa) | Incoloy 925: 695, Inconel 625: 914 |
| Tensile Strength (FSW at 30 mm/min) | 685 MPa |

## 4.0 Conclusion

This study successfully demonstrated the feasibility of joining Incoloy 925 and Inconel 625, two critical high-temperature alloys, using the FSW process. A comprehensive investigation was conducted to optimize process parameters and characterize the resulting weld joints.

1. A process window was established with optimal welding speeds of 20-30 mm/min at a constant tool rotation speed of 400 rpm, resulting in robust joints.
2. Microstructural analysis revealed distinct zones within the weld, including the base metal, a minimal HAZ, the TMAZ, and the SZ.
3. The FSW process did not induce any significant phase changes or oxidation in either alloy.
4. Microhardness measurements showed a gradual increase in hardness from the base metal towards the SZ, attributed to grain refinement.
5. Tensile testing indicated that Inconel 625 exhibits higher strength compared to Incoloy 925.
6. While demonstrating good strength, the weld displayed limited ductility, likely due to the inherent differences in the deformation behavior of the dissimilar alloys.

This study provides valuable insights into the feasibility and characteristics of FSW joints between these high-performance alloys, contributing to the advancement of joining technologies for high-temperature applications.

## 5.0 Acknowledgment

The authors extend their gratitude to the Koneru Lakshmaiah Education Foundation in Guntur, for furnishing the necessary resources to conduct this research. Additionally, the authors appreciate the support from the Central Analytical Laboratory at BITS Hyderabad for access to the PXRD facility.

## 6.0 References

1. Karim MA, Park Y. A review on welding of dissimilar metals in car body manufacturing. J Weld Join. 2020; 38(1):8-23. https://doi.org/10.5781/JWJ.2020.38.1.1
2. Lee S, Moon J, Kim H, Cho YH, Lee HH, Choi H, *et al*. Development of functionally graded austenitic lightweight steel through electrically assisted pressure solid-state joining. Mater Sci Eng A. 2024; 891:146003. https://doi.org/10.1016/j.msea.2023.146003
3. Zhang S, Loi TV, Boakye SY, Anaman SY, Cai L, Gao K, *et al.* Effectiveness of an additively manufactured porous layer in dissimilar solid-state bulk joining of additively manufactured maraging steel and conventional AISI410 steel. Addit Manuf. 2022; 49:102508. https://doi.org/10.1016/j.addma.2021.102508
4. Grong O, Sandnes L, Berto F. Progress in solid state joining of metals and alloys. Procedia Struct Integr. 2019; 17:788-798. https://doi.org/10.1016/j.prostr.2019.08.105
5. Hong S, Li Y, Park J, Han HN. Effectiveness of electrically assisted solid-state pressure joining using an additive manufactured porous interlayer. CIRP Ann Manuf Technol. 2018; 67(1):297-300. https://doi.org/10.1016/j.cirp.2018.04.062
6. Devaraju A, Shalem MJ, Manichandra B. Effect of rotation speed on tensile properties and microhardness of dissimilar Al alloys 6061-T6 to 2024-T6 welded via solid state joining technique. Mater Today Proc. 2019; 18:3286-3290. https://doi.org/10.1016/j.matpr.2019.07.235
7. Manjhi SK, Das A, Prasad SB. Review on joining of aluminum alloy by solid-state welding technique. Mater Today Proc. 2020; 26:1255-1261. https://doi.org/10.1016/j.matpr.2020.02.251
8. Miriyev A, Barlam D, Shneck R, Stern A, Frage N. Steel to titanium solid state joining displaying superior mechanical properties. J Mater Process Technol. 2014; 214(12):2884-2890. https://doi.org/10.1016/j.jmatprotec.2014.06.026
9. ESayed MM, Shash AY, Abd-Rabou M, ElSherbiny MG. Welding and processing of metallic materials by using friction stir technique: A review. J Adv Joining

Process. 2021; 3:100059. https://doi.org/10.1016/j.jajp.2021.100059
10. Khaliq UA, Muhamad MR, Yusof F, Ibrahim S, Isa MSM, Chen Z, *et al.* A review on friction stir butt welding of aluminum with magnesium: A new insight on joining mechanisms by interfacial enhancement. J Mater Res Technol. 2023; 27:4595-4624. https://doi.org/10.1016/j.jmrt.2023.10.158
11. Ma L, Xu Z, Zhang T, Chen G, Sun S, Zhou L, *et al. In-situ* formed amorphous phase in aluminum/steel friction stir welds: Interface evolution and strength improvement. J Adv Joining Process. 2024; 9:100220. https://doi.org/10.1016/j.jajp.2024.100220
12. Prabhu L, Shanmugam S, Chandrasekaran T. Effect of tool pin profiles over square wave tool path pattern on friction stir welding of AA6061-Cu dissimilar alloys. Mater Technol. 2021; 55(6):693-700. https://doi.org/10.17222/mit.2021.202
13. Ahmed MMZ, Seleman MM, Fydrych D, Cam G. Review on friction stir welding of dissimilar magnesium and aluminum alloys: Scientometric analysis and strategies for achieving high-quality joints. J Magnes Alloy. 2023; 11(11):4082-4127. https://doi.org/10.1016/j.jma.2023.09.039
14. Isa MSM, Moghadasi K, Ariffin MA, Raja S, Muhamad MR, Yusof F, *et al.* Recent research progress in friction stir welding of aluminum and copper dissimilar joint: a review. J Mater Res Technol. 2021; 15:2735-2780. https://doi.org/10.1016/j.jmrt.2021.09.037
15. Zhao W, Zhu Y, Yi X, Zhai M, Zhao K, Wang F, *et al.* Influence mechanism of pin length and shape on the heat-flow field of Al/Cu friction stir lap welding. Mater Today Commun. 2024; 40:109459. https://doi.org/10.1016/j.mtcomm.2024.109459
16. Singh VP, Patel SK, Ranjan A, Kuriachen B. Recent research progress in solid-state friction-stir welding of aluminum-magnesium alloys: a critical review. J Mater Res Technol. 2020; 9(6):6217-6256. https://doi.org/10.1016/j.jmrt.2020.01.008
17. Panaskar N, Terkar R. A review on recent advances in friction stir lap welding of aluminum and copper. Mater Today Proc. 2017; 4:8387-8393. https://doi.org/10.1016/j.matpr.2017.07.182
18. Ambrosio D, Morisada Y, Ushioda K, Fujii H. Material flow in friction stir welding: A review. J Mater Process Technol. 2023; 320:118116. https://doi.org/10.1016/j.jmatprotec.2023.118116
19. Gupta RK, Kumar VA, Gururaja UV, Shivaram BRNV, Prasad YM, Ramkumar P, *et al.* Processing and characterization of Inconel 625 Nickel base superalloy. Mater Sci Forum. 2015; 830:38-40. https://doi.org/10.4028/www.scientific.net/MSF.830-831.38
20. Su G, Shi Y, Li G, Zhang G, Xu Y. Highly efficient additive manufacturing of Inconel 625 thin wall using hot-wire laser metal deposition: Process optimization, microstructure, and mechanical properties. Opt Laser Technol. 2024; 175:110763. https://doi.org/10.1016/j.optlastec.2024.110763
21. DuPont JN, Lippold JC, Samuel KD. Welding metallurgy and weldability of Nickel-base alloys. Hoboken: Wiley; 2009. https://doi.org/10.1002/9780470500262
22. Lemke TF, Harris JA. High-alloy materials for offshore applications. Presented at the 15th Annual OTC, Houston, Texas; 1983. https://doi.org/10.4043/4451-MS
23. Herrera-Chavez LY, Ruiz A, Lopez-Morelos VH, Rubio-Gonzalez C. Microstructural characterization and mechanical response of Inconel 600 welded joint. Mater Charact. 2019; 157:109882. https://doi.org/10.1016/j.matchar.2019.109882
24. Song KH, Nakata K. Mechanical properties of friction-stir-welded Inconel 625 alloy. Mater Trans. 2009; 50(11):2498-2501. https://doi.org/10.2320/matertrans.M2009200
25. Komarasamy M, Smith C, Darsell J, Choi W, Jana S, Grant G. Microstructure and mechanical properties of friction stir welded Haynes 282. Mater Charact. 2021; 182:111558. https://doi.org/10.1016/j.matchar.2021.111558
26. Prakash E, Chandrasekar G, Krishnan BR, Ramesh M, Sundaresan R. Investigate the welding of Inconel 718 and Inconel 600 in friction stir welding. Mater Today Proc. 2022; 60:1385-1388. https://doi.org/10.1016/j.matpr.2021.10.305
27. Ghailane A, Oluwatosin AO, Larhlimi H, Hejjaj C, Makha M, Busch H. Titanium nitride, TiXN(1−X), coatings deposited by HiPIMS for corrosion resistance and wear protection properties. Appl Surf Sci. 2022; 574:151635. https://doi.org/10.1016/j.apsusc.2021.151635